60-YEAR Remote Sensing Observations Revealed Cross-Cycle Evolution of the Brunt Ice Shelf in the Context of Global Warming

Cheng, Yuan; Xue, Jiamei; Yu, Haomin; Hai, Gang

Published in:
ISPRS Annals of the Photogrammetry, Remote Sensing and Spatial Information Sciences

DOI (link to publication from Publisher):
10.5194/isprs-archives-XLVIII-4-W9-2024-99-2024

Publication date:
2024

Document Version
Publisher's PDF, also known as Version of record

60-YEAR REMOTE SENSING OBSERVATIONS REVEALED CROSS-CYCLE EVOLUTION OF THE BRUNT ICE SHELF IN THE CONTEXT OF GLOBAL WARMING

Y. Cheng [1,2], J. Xue [1,2], H. Yu [3 *], G. Hai [4,5 *]

[1] Institute for the Conservation of Cultural Heritage, School of Cultural Heritage and Information Management, Shanghai University, Shanghai, China – chengyuan@shu.edu.cn, xjmshu@shu.edu.cn
[2] Key Laboratory of Silicate Cultural Relics Conservation (Shanghai University), Ministry of Education – chengyuan@shu.edu.cn, xjmshu@shu.edu.cn
3 Department of Computer Science, Aalborg University, Aalborg, Denmark – haominyu@cs.aau.dk
[4] Dept. of College of Surveying and Geo-Informatics, Tongji University, Shanghai, China – ganghaitj@gmail.com
[5] Mogo Auto Intelligence and Telematics Information Technology Company Ltd., Beijing 100013,China – ganghaitj@gmail.com

KEY WORDS: Remote Sensing, Global Climate Change, Antarctic Ice Sheet, Ice Shelves.

ABSTRACT:

The Antarctic Ice Sheet (AIS) holds the potential to raise global sea levels by a staggering 57 m. Ice shelves, extensions of these ice sheets into the ocean, play a crucial role in stabilizing the upstream ice sheet. The Brunt Ice Shelf (BIS), located in the Southern Weddell Sea region and proximal to the continental shelf break, stands as a vital indicator for the region's response to global climate warming. Hence, this study systematically employs a range of remote sensing and field data, including remote sensing data from 1963 to 2023 (ARGON images, Landsat1-9 images, Sentinel-1 images, ICESat-2 altimetry data, etc.) and in-situ ice flow velocity data since 1956, to conduct a comprehensive analysis of the BIS's calving cycle and evolution over nearly six decades. The results reveal a significant exacerbation of both dynamical and structural instabilities in the BIS compared to the calving cycle in the 1970s. Combining analyses of air temperature from meteorological station, water temperature from ocean models and in-situ measurements such as Conductivity-Temperature-Depth profiles, the study suggests that the increased instability of the BIS is likely linked to the intrusion of warmer currents over the continental shelf. This research provides valuable insights into the evolving behavior of the BIS in response to changing climate conditions, underscoring the critical role of remote sensing data in advancing our understanding of these processes on a global scale.

1. INTRODUCTION

The Intergovernmental Panel on Climate Change (IPCC) Sixth Assessment Report highlights that from 1850–1900 to 2006–2015, human activities have resulted in a global average temperature increase of 0.87±0.12°C. Against this backdrop, the melting of ice sheets and glaciers has emerged as a primary contributor to the rise in global sea levels. The Antarctic Ice Sheet (AIS) represents the Earth's largest block of ice, and a complete melt has the potential to contribute to a staggering 57 m of global sea level rise (Rignot et al., 2019). Ice shelves, extensions of the ice sheet into the ocean, play a crucial role in protecting the inland ice sheet (Rignot et al., 2013). The loss of mass from ice shelves, primarily through processes such as iceberg calving and basal melting (Depoorter et al., 2013; Liu et al., 2015; Rignot et al., 2013), leads to the subsequent acceleration of ice discharge from both ice sheets and glaciers across the grounding line. This acceleration results from the diminishing buttressing effect (Cheng et al., 2021; Fürst et al., 2016)(Scambos et al., 2004; Dupont et al., 2005; Fürst et al., 2016). The complex interplay of the ice sheet, ice shelves, and the ocean collectively determines the stability of the ice sheet and its contribution to sea-level rise. Therefore, understanding the response characteristics of the AIS and its surrounding ice shelves to global climate change is paramount for precise assessment and prediction of their impact on global sea levels (Cheng et al., 2021).

The calving cycle of Antarctic ice shelves often spans several decades. Within a single cycle, natural processes occur, including the advance and retreat of the grounding line and variations in flow velocity. If the research timeframe is not sufficiently extended, the observed changes in instability may represent natural variations within the calving cycle rather than indicative of the long-term evolutionary trend of the Antarctic ice sheet under the influence of climate change (Cheng et al., 2021; Li et al., 2023).

The Brunt Ice Shelf (BIS) is situated near the Coats Land, East Antarctica. As early as 1956, the British Antarctic Survey (BAS) established a ground observation network on the BIS for continuous monitoring of the ice shelf's changes (De Rydt et al., 2019; Hodgson et al., 2019). The establishment of this network has provided an opportunity for us to comprehensively utilize multi-source data, analyze the long-term evolution characteristics of the ice shelf's instability, and gain insights into the impact of global climate change on Antarctic ice shelves. The results from ground observations indicate that the ice flow velocity at several GPS stations on the BIS remained stable for nearly three decades. However, a notable acceleration of approximately 10% per year was observed during the period from 2012 to 2016, signifying a significant departure from the preceding stable phase(Gudmundsson et al., 2017). This acceleration was interpreted as an indication of increased instability. In February 2021, BIS underwent a significant calving event, releasing an approximately 1,270 km^2 iceberg

* Corresponding author

(https://www.bas.ac.uk/project/brunt-ice-shelf-movement/), and on January 23, 2023, another massive iceberg measuring 1,550 km² broke off from the BIS (https://www.bas.ac.uk/media-post/brunt-ice-shelf-in-antarctica-calves-giant-iceberg/). Various indicators suggest that the evolutionary pattern of BIS may have undergone some changes in the past few decades. Nevertheless, there remains a dearth of comprehensive research on the evolution of BIS, leaving uncertain whether they are part of the natural calving cycle or manifestations of exacerbated instability under the influence of climate change.

In this study, the dynamic and structural characteristics of the BIS were investigated using remote sensing data and field data spanning nearly 60 years. Leveraging a series of ice flow velocity maps and on-site observational data from ground stations, we analyzed the dynamic changes in the ice shelf. Combining altimetry data with satellite imagery, we examined the geometric structure of BIS and the evolving features of critical ice surface rifts. Additionally, long-term meteorological data, ocean models, and Conductivity-Temperature-Depth (CTD) profiles were utilized to explore the potential relationships between air and water temperatures and the stability of BIS.

2. STUDY SITE

BIS is situated in West Antarctica, with geographical coordinates ranging from 22°W to 30°W and 74°S to 76°S. As the ice sheet from Coats Land advances over grounded-line cliffs, it descends into the sea, giving rise to small icebergs that swiftly amalgamate with sea ice, forming the heterogeneous ice shelf known as BIS. Positioned on the northeastern flank of the Antarctic's second-largest ice sheet, the Filchner-Ronne Ice Shelf, BIS stands among the ice shelves nearest to the continental shelf break in the Weddell Sea Sector. ~210 km from the grounding line, the BIS ice shelf features a pivotal regrounding point—McDonald Ice Rumples (MIR)—providing a stabilizing buttressing to the ice shelf.

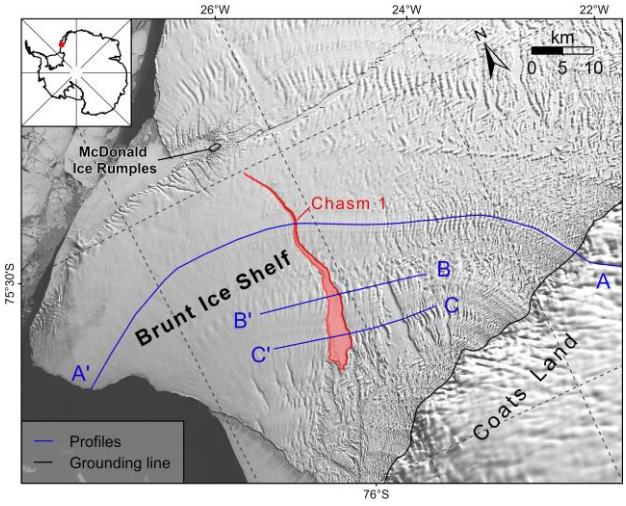

Figure 1. Map of Brunt Ice Shelf with a thumbnail in the upper left corner shows the location of the ice shelf. Black line shows the location of the grounding line (Rignot et al., 2011a), red polygon represents the location of Chasm 1, blue lines along the ice flow lines illustrate the locations of three profiles, overlaid on a Landsat-8 OLI image of 24 September 2020.

3. DATASET AND METHODS

3.1 Remote Sensing data

3.1.1 Satellite Images: To facilitate continuous long-term observations of the BIS, we employed multi-source satellite imagery spanning from 1963 to the present. Digitalization and measurements were conducted on the geometric morphology of the ice shelf and key rifts on the ice shelf.

Data	Temporal coverage	Spatial resolution	Data format
ARGON	1963/10/29	33	GeoTIFF
Landsat-1 MSS	1974/01/27	60	GeoTIFF
Landsat-7 ETM+	2012/11/13	15	GeoTIFF
Landsat-7 ETM+	2013/02/01	15	GeoTIFF
Landsat-8 OLI	2013/12/03	15	GeoTIFF
Landsat-8 OLI	2014/01/04	15	GeoTIFF
Landsat-8 OLI	2014/12/15	15	GeoTIFF
Landsat-8 OLI	2015/01/07	15	GeoTIFF
Landsat-8 OLI	2015/12/09	15	GeoTIFF
Landsat-8 OLI	2016/01/01	15	GeoTIFF
Landsat-8 OLI	2016/12/11	15	GeoTIFF
Landsat-8 OLI	2017/01/28	15	GeoTIFF
Landsat-8 OLI	2017/12/21	15	GeoTIFF
Landsat-8 OLI	2018/03/11	15	GeoTIFF
Landsat-8 OLI	2018/09/28	15	GeoTIFF
Landsat-8 OLI	2019/01/18	15	GeoTIFF
Landsat-8 OLI	2019/11/02	15	GeoTIFF
Landsat-8 OLI	2020/01/05	15	GeoTIFF
Landsat-8 OLI	2020/10/19	15	GeoTIFF
Sentinel-1 GRD	2021/02/25	~40	GeoTIFF
Sentinel-1 GRD	2021/03/06	~40	GeoTIFF
Landsat-9 OLI-2	2023/01/21	15	GeoTIFF
Landsat-8 OLI	2023/02/05	15	GeoTIFF

Table 1. Remote sensing images used in this study, including ARGON, Landsat-1 MSS, Landsat-7 ETM+, Landsat-8 OLI , Sentinel-1 GRD, and Landsat-9 OLI-2 images.

The width of the rift is defined along the profiles BB' and CC' (Figure 1), while the length of the rift is measured along the central line of Chasm 1 from south to north. The measurement error for the results is approximately 1 pixel.

3.1.2 Elevation data: An analysis of the elevation changes of the BIS was conducted based on the basal melting rates from 2010 to 2018 and surface elevation changes from 2019 to 2020. Firstly, the average melting rate on the BIS for the years 2010-2018 was extracted using the Antarctic ice shelf melt rates product. This product has a resolution of 500 m and is reported to possess high accuracy(Adusumilli et al., 2020).

Furthermore, this study estimated the surface elevation changes of the ice shelf during the period 2019 to 2020 using ICESat-2 ATL11 Annual Land Ice Height (Version 3) data. The ATL11 dataset is derived from ICESat-2 ATL06 Land-Ice Height product data(Smith et al., 2019; Smith et al., 2021). After filtering the data using the quality label 'quality_summar,' the surface

elevation change rate was estimated by fitting the linear trend of the ATL11 surface elevation time series. Additionally, elevation points within 5 m of mean sea level or with elevation change rates exceeding 2 m per year were likely situated within rifts and were therefore removed to avoid influencing the results. Moreover, only the results of elevation changes within the flat region of the ice shelf were considered in this study.

3.1.3 Ice flow velocity products: To capture the spatiotemporal distribution of ice flow velocity on the ice shelf, two ice flow velocity products were employed in this study. These include the MEaSUREs Annual Velocity Map v1 with a time span from 2005 to 2017 (Mouginot et al., 2017; Rignot et al., 2011b) and the ITS_LIVE Annual Velocity Map covering the period from 1985 to 2018(Gardner et al., 2019). Additionally, using the autoRIFT v1 software(Gardner et al., 2018), surface velocity maps for the BIS in 2019, 2020, and 2021 were calculated.

Velocity profiles at different time periods were generated along profile AA', located at the center of the ice shelf (Figure 1). Considering the resolution of the velocity maps as 240 m, the sampling interval along the profiles was set to 240 m as well. Specifically, to visually depict the temporal variation trend of the BIS's velocity, the mean velocity for a segment near the ice shelf's front was calculated for each profile, generating a time series of ice flow velocities.

3.2 Meteorological data

3.2.1 Air temperature: In terms of air temperature, records from the Halley Station were gathered in this study to obtain temperature observation data on the BIS (https://www.bas.ac.uk/polar-operations/sites-and-facilities/facility/halley/).

3.2.2 Water temperature: Simulations of sea water temperature near the front of the BIS were conducted based on the GECCO3 (German contribution to the Estimating the Circulation and Climate of the Ocean project) ocean synthesis (Köhl, 2020). According to the ocean bathymetry data from BedMachine, the continental shelf near the frontal edge of the BIS has elevations ranging from -500 to -200 m(Morlighem et al., 2020). Therefore, in this study, sea water temperatures were calculated using the GECCO3 ocean model within the range of 6 to 362.5 m depth. The average temperature in the region of 24–29°W and 75–76°S for each month was obtained by averaging all simulated values within this depth and spatial range.

In addition, to validate the calculated sea water temperatures in the model, this study compiled CTD data from the EN4 observational dataset (Good et al., 2013) during the research period.

4. RESULTS

4.1 Dynamic evolution of BIS

Based on the above data and methods, the dynamic evolution characteristics of the BIS were analyzed.

The earliest observations of flow velocity on the BIS date back to the establishment of the Halley Station in 1956. Gudmundsson et al. (2017)analyzed ice flow velocity on the BIS based on observational data from the Halley Station. As shown in Figure 2a and b, on the northern flank of the BIS, there was a calving event in the early 1970s. Before the calving event in the early 1970s, the ice flow velocity remained at a relatively low level. Following the calving on the northern flank, the velocity on the ice shelf rapidly increased as the connection between the BIS and the MIR was lost, and the support from MIR to the upstream ice shelf ceased. Subsequently, as the ice shelf gradually moved forward, reconnecting with the MIR, MIR resumed providing support to the ice shelf. Therefore, the velocity decreased gradually with the increasing contact area between the ice shelf and the MIR.

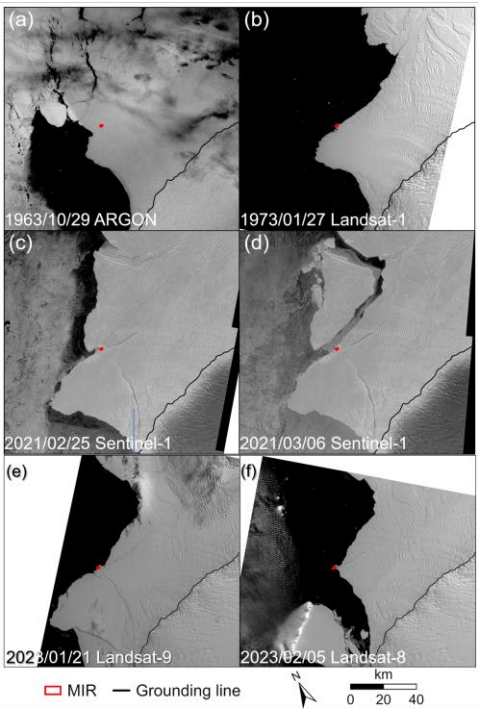

Figure 2. Changes of the BIS ice front. (a) and (b) are images of 1963 and 1973 used to represent the calving in 1970s at the northern flank of the BIS; (c) and (d) are images of February 25 and March 6, 2021 used to represent the calving in 2021 at the northern flank of the BIS, the western flank of BIS did not experience significant retreat. The red polygon is MIR and the black line is grounding line fromRignot et al. (2011a).

Until 2012, the flow velocity of the BIS began to change once again. As shown in Figure 3, spatially, there is relatively small variability in flow velocity in the inland areas, while at the front of the ice shelf, the flow velocity exhibits larger fluctuations over time. Temporally, the ice flow velocity remained relatively stable during the period from 2013 to 2016, but significant changes occurred after 2016. The most substantial fluctuation in ice flow velocity during the study period occurred in 2018 and 2019. Specifically, the average velocity in 2013 was 393±10 m/y, increased by ~90 m/y in 2014, and remained constant for the following year. Subsequently, from 2015 to 2019, the average velocity increased year by year, reaching 811±35 m/y in 2019. After a slight decrease in 2020, it increased again to 819±10 m/y in 2021.

As shown in Figure 2c and d, in February 2021, the western flank of the BIS underwent a significant calving event, releasing an approximately 1,270 km² iceberg A-74. Subsequently, based on continuous GPS observations from the Halley Research Station, BIS has been in a sustained acceleration state. During the period from 2021 to early 2023, the average acceleration observed by GPS was 54 m/y² (Marsh et al., 2023). By January 2023, as depicted in Figure 2e and f, the western flank of BIS experienced

another calving event, with an approximately 1,500 km² iceberg, A-81, detaching. Following this event, the ice shelf's velocity underwent further acceleration. According to the results from Marsh et al. (2023), the average acceleration observed by GPS from January to July 2023 was 490 m/y². Subsequently, in July 2023, a small calving event with an area of approximately 0.25 km² occurred at the front of BIS. Following this event, the average acceleration surged to 1,705 m/y² (Marsh et al., 2023).

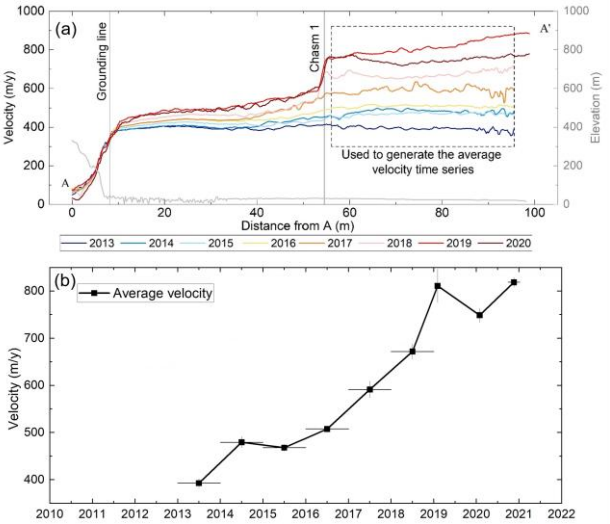

Figure 3. (a) Ice flow velocity from 2013 to 2020 along profile AA', and (b) time series of the average ice flow velocity calculated using the values within the dashed box in (a).

One noteworthy observation is that, unlike the previous acceleration event, there has been a significant increase in the flow velocity on the BIS since 2013. Prior to this, no calving events had occurred at the front of the ice shelf, indicating that the acceleration occurred significantly earlier than the calving event on the northern flank of the BIS in February 2021. There were no observed acceleration signals before the last calving event. This suggests that the BIS is currently more active than in the previous cycle.

4.2 Structural evolution of BIS

Based on the previously mentioned data and methods, the structural evolution characteristics of the BIS were analyzed.

4.2.1 Calving of BIS: Firstly, this study analyzed the long-term geometric evolution characteristics of the BIS from 1963 to the present based on collected multi-source satellite images. As Figure 2 indicates, the earliest image that can be used to observe the front of BIS is an ARGON image collected in 1963. Combining with a Landsat-1 image taken in 1973, the changes in the ice front of BIS in the early 1970s were observed. The images of 1963 and 1973 were geophysical registered to a Landsat-8 image of 2021. As Figure 2a and b suggested, a calving event took place in northern flank of the BIS, while the western flank of BIS did not experience significant retreat. Thereafter, the ice front of BIS advanced gradually, reaching its most forward position since 1963. In February 26, 2021, another calving event occurred at the north of MIR, resulting an area loss of 1,270 km^2. Two years later, the western part of BIS experienced another calving event, as shown in Figure 2e and f. This calving event resulted in an ice shelf area loss of approximately 1,500 km^2.

In summary, since 1963, the western side of the BIS has experienced a calving event in 2023, while the northern flank of BIS underwent two similar events in the early 1970s and 2021, respectively. These occurrences provide a unique opportunity to investigate the behavior of BIS both before and after calving events.

4.2.2 Propagation of Chasm 1: Next, these remote sensing images were further utilized for continuous monitoring of the critical rift, Chasm 1, on the BIS. Considering that the propagation of Chasm 1 was essentially stagnant before 2012, the measurement results presented here are from 2013 onwards.

Starting from 2013, the length of Chasm 1 has been steadily increasing, eventually contributing to the calving of the BIS. The growth of Chasm 1 has been characterized by an uneven pace. As depicted in Figure 4, from 2013 to 2017, the northern tip of Chasm 1 was traversing the suture zone of the ice shelf (Hulbe et al., 2010). Due to significant heterogeneity in ice properties near the suture zone, with notable differences in mechanical and physical characteristics, the growth of Chasm 1 was constrained, resulting in minimal length changes. However, during this period, stress gradually accumulated until it could overcome the resilience of the ice material. Hence, after 2017, Chasm 1 initiated rapid expansion, with an average growth rate of 6.97 km/y from 2017 to 2019. By November 2, 2019, after this period of rapid growth, the length of Chasm 1 reached 37.95 km, entering a subsequent phase of very slow expansion.

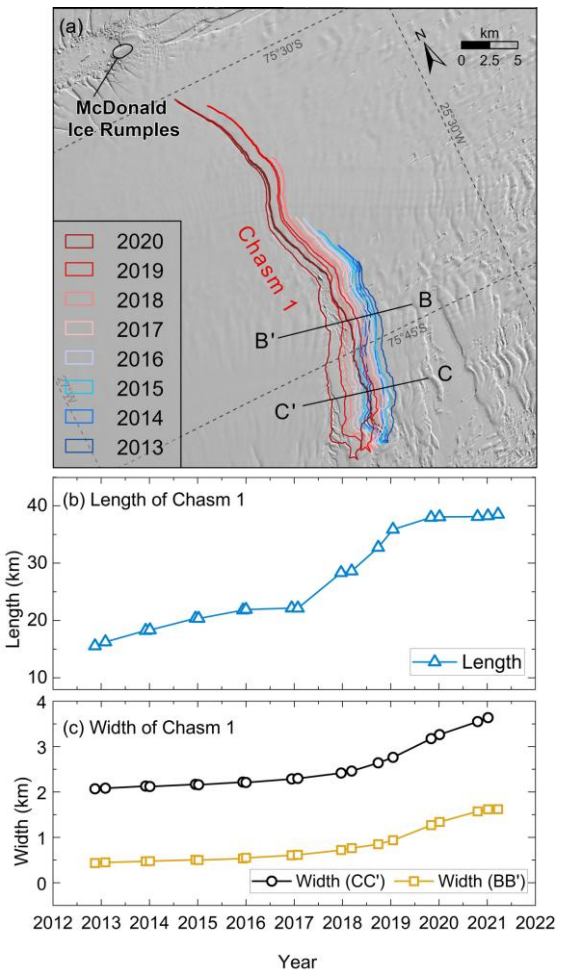

Figure 4. (a) The different-colored polygons illustrate the Position and shape of Chasm 1 from 2013 to 2020, (b) The Time

series of the length and width of Chasm 1 obtained from measurements based on remote sensing images.

Given that the variations in the length of Chasm 1 may be influenced by the physical characteristics of the ice shelf itself, such as the suture zone, which could impact the accuracy of our analysis of stability changes over time. Therefore, along profiles BB' and CC', the width of Chasm 1 was also measured in this study. As depicted in Figure 4c, the trends in width changes at both locations are essentially consistent, indicating that the width of the rift is a good indicator of ice shelf stability. Specifically, on November 11, 2012, the width along profile BB' was 0.43 km, and after 5 years, it increased by 0.29 km, with a relatively slow widening rate of only 0.06 km/y. However, after December 21, 2017, the widening rate of Chasm 1 suddenly accelerated to 0.30 km/y. The width along profile CC' exhibited a similar changing pattern. In fact, as mentioned earlier, the growth rate of Chasm 1's length also significantly increased after 2017. The rapid expansion of Chasm 1 in both length and width laid the groundwork for the calving event A-81 in early 2023.

4.2.3 Elevation changes: The study utilized the Antarctic ice shelf melt rates product provided by Adusumilli et al. (2020) to calculate the average melt rates of the BIS during the period from 2010 to 2018. Additionally, surface height changes for the years 2019 to 2020 were estimated using data from ICESat-2 ATL11 Annual Land Ice Height (Version 3). The analysis specifically focused on the height change results near the shelf front, particularly in areas where the topography is relatively flat. During the period from 2010 to 2018, the ice shelf exhibited a notable positive basal melt rate, with an average melting velocity of 1.02±0.42 m/y at the front of ice shelf. In the subsequent period of 2019–2020, there was a discernible downward trend in surface elevation, with an average speed of -0.39±0.43 m/y.

5. DISSCUSSIONS

Building upon the long-term observations discussed in Section 4.2, both the dynamical and structural characteristics of the BIS have undergone changes in recent decades, suggesting a potential increase in its instability. Therefore, this study further analyzes the trends in air temperature and sea water temperature in the region to unravel the underlying causes of the recent changes observed in BIS.

5.1 Air temperature

To further investigate the connection between the evolution of the BIS and climate change, this study generated a time series of temperature based on the data from Halley Station for the years 2012−2020, as depicted by the light grey line in Figure 5a. Additionally, to emphasize the interannual trends in temperature changes, a 12-month moving average filter was applied to the temperature data, as illustrated by the black line in Figure 5a.

Overall, the temperatures in the region remained stable around -20°C, with the coldest monthly temperatures hovering around -30°C, and even the warmest monthly temperatures remaining below 0°C. Such extremely low temperatures are generally not conducive to inducing instability in the ice shelf. Therefore, air temperature may not be the primary driver of the changes occurring in BIS.

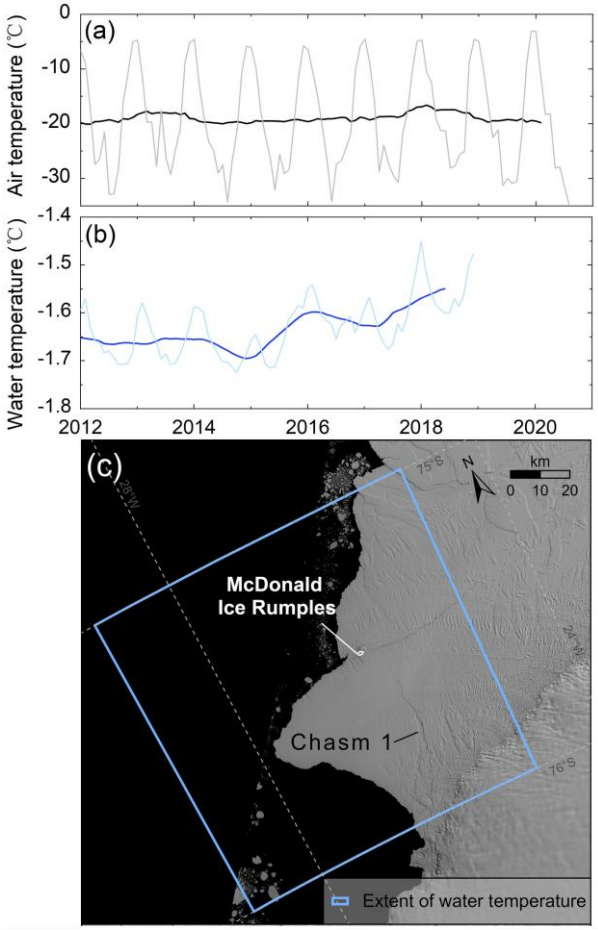

Figure 5. Time series of (a) air temperature at Halley Station, with the light grey line representing the raw data and the black line representing the 12-month moving average; (b) water temperature calculated based on the GECCO3 model, with the light blue line representing the raw data and the blue line representing the 12-month moving average; and (c) spatial range for calculating the water temperature in (b).

5.2 Water temperature:

In this study, the sea water temperature at the front of the BIS was simulated using the GECCO3 model. As shown in Figure 5b, the temperature corresponding to each time represents the average temperature within the blue box range in Figure 5c. Similar to the approach used for air temperature data, a 12-month moving average was applied to highlight the long-term trends in sea water temperature in the region, minimizing the impact of seasonal variations on the results. The findings indicate that from early 2012 to the end of 2014, the sea water temperature remained relatively stable, with an average of -1.66°C. Starting from early 2015, the sea water temperature began to show a fluctuating upward trend. The temperature gradually increased, reaching -1.55°C by the end of 2018 (see Figure 5b).

On the other hand, the presence of warm water near the bottom of the continental shelf in February 2017 is evident (Ryan et al., 2020). CTD profiles at the front of the BIS reveal a significant temperature increase beyond 250 m depth, with the highest observed water temperature of -0.6°C at a depth of 400 m. This alignment between observed sea water temperature data and ocean models indicates a consistent warming trend in the bottom waters of this region.

Correspondingly, after 2016, there is a noticeable increase in the ice flow velocity at the front of the ice shelf (Figure 3). The expansion rates of Chasm 1, both in terms of length and width, have significantly accelerated as well (Figure 4). Additionally, the thickness of the ice shelf has been consistently decreasing. Based on these observations, it can be inferred that the warm water observed on the continental shelf near the BIS might be one of the contributing factors to the thinning of the ice shelf.

6. CONCUSSIONS

In this study, we conducted extensive observations and analyses of the BIS over several decades to comprehend its dynamic and structural evolution, as well as its potential correlation with climate change and ocean conditions. By analyzing nearly 60 years of remote sensing data, we observed the temporal and spatial dynamics of BIS, with a particular focus on ice flow velocity, geometric changes, and the evolution of critical rifts. During the period from 2013 to 2021, the ice flow velocity at the front of BIS more than doubled. The acceleration in ice flow velocity became more pronounced after the calving events on the northern and western flanks of the ice shelf in 2021 and 2023, respectively. This increased instability in the ice shelf, characterized by accelerated ice flow, contrasts with the previous calving event in the early 1970s when ice flow acceleration occurred post-calving. Chasm 1 exhibited significant expansion from 2013 to 2020, setting the stage for subsequent ice shelf calving events. The thickness of BIS continued to decrease from 2010 to 2020. To investigate the variations in air temperature and sea water temperature around BIS, we utilized meteorological station data and ocean model simulations. A notable rise in sea water temperature on the continental shelf near BIS since 2015 was observed, likely being one of the primary reasons contributing to the thinning and increased instability of the ice shelf. These findings are pivotal for gaining a deeper understanding of Antarctic ice shelf responses to climate change and their implications for future sea-level rise.

ACKNOWLEDGEMENTS

This research was supported by the National Science Foundation of China (42301149) and research project of Shanxi Cultural Relics Bureau (2024KT19).

REFERENCES

Adusumilli S., Fricker H. A., Medley B., Padman L., Siegfried M. R. 2020: *Interannual variations in meltwater input to the Southern Ocean from Antarctic ice shelves*. Nat Geosci ;13:616-20. doi.org/10.1038/s41561-020-0616-z.

Cheng Y., Xia M., Qiao G., Li Y., Hai G., Lv D. 2021: *Calving cycle of Ninnis Glacier over the last 60 years*. Int J Appl Earth Obs Geoinf ;105:102612. doi.org/10.1016/j.jag.2021.102612.

De Rydt J., Gudmundsson G. H., Nagler T., Wuite J. 2019: *Calving cycle of the Brunt Ice Shelf, Antarctica, driven by changes in ice shelf geometry*. The Cryosphere ;13:2771-87. doi.org/10.5194/tc-13-2771-2019.

Depoorter M. A., Bamber J. L., Griggs J. A., Lenaerts J. T. M., Ligtenberg S. R. M., van den Broeke M. R., Moholdt G. 2013: *Calving fluxes and basal melt rates of Antarctic ice shelves*. Nature ;502:89-92. doi.org/10.1038/nature12567.

Fürst J. J., Durand G., Gillet-Chaulet F., Tavard L., Rankl M., Braun M., Gagliardini O. 2016: *The safety band of Antarctic ice shelves*. Nat Clim Chang ;6:479-82. doi.org/10.1038/nclimate2912.

ITS_LIVE Regional Glacier and Ice Sheet Surface Velocities. https://its-live.jpl.nasa.gov/, 2019(accessed 2021/7/14).

Gardner A. S., Moholdt G., Scambos T., Fahnstock M., Ligtenberg S., van den Broeke M., Nilsson J. 2018: *Increased West Antarctic and unchanged East Antarctic ice discharge over the last 7 years*. The Cryosphere ;12:521-47. doi.org/10.5194/tc-12-521-2018.

Good S. A., Martin M. J., Rayner N. A. 2013: *EN4: Quality controlled ocean temperature and salinity profiles and monthly objective analyses with uncertainty estimates*. Journal of Geophysical Research: Oceans ;118:6704-16. doi.org/10.1002/2013JC009067.

Gudmundsson G. H., De Rydt J., Nagler T. 2017: *Five decades of strong temporal variability in the flow of Brunt Ice Shelf, Antarctica*. J Glaciol ;63:164-75. doi.org/10.1017/jog.2016.132.
Hodgson D. A., Jordan T. A., De Rydt J., Fretwell P. T., Seddon S. A., Becker D., Hogan K. A., Smith A. M., Vaughan D. G. 2019: *Past and future dynamics of the Brunt Ice Shelf from seabed bathymetry and ice shelf geometry*. The Cryosphere ;13:545-56. doi.org/10.5194/tc-13-545-2019.

Hulbe C. L., LeDoux C., Cruikshank K. 2010: *Propagation of long fractures in the Ronne Ice Shelf, Antarctica, investigated using a numerical model of fracture propagation*. J Glaciol ;56:459-72. doi.org/10.3189/002214310792447743.

Köhl A. 2020: *Evaluating the GECCO3 1948–2018 ocean synthesis – a configuration for initializing the MPI-ESM climate model*. Q J R Meteorol Soc ;146:2250-73. doi.org/10.1002/qj.3790.

Li R., Cheng Y., Chang T., Gwyther D. E., Forbes M., An L., Xia M., Yuan X., Qiao G., Tong X., Ye W. 2023: *Satellite record reveals 1960s acceleration of Totten Ice Shelf in East Antarctica*. Nat Commun ;14. doi.org/10.1038/s41467-023-39588-x.

Liu Y., Moore J. C., Cheng X., Gladstone R., Bassis J. N., Liu H., Wen J., Hui F. 2015: *Ocean-driven thinning enhances iceberg calving and retreat of Antarctic ice shelves*. Proc Natl Acad Sci U S A ;112:3263-8.

Marsh L. J., Luckman A. J., Hodgson D. A. 2023: *Brief Communication: Rapid acceleration of the Brunt Ice Shelf after calving of iceberg A-81*. EGUsphere [preprint]. doi.org/10.5194/egusphere-2023-1949.

Morlighem M., Rignot E., Binder T., Blankenship D., Drews R., Eagles G., Eisen O., Ferraccioli F., Forsberg R., Fretwell P., Goel V., Greenbaum J. S., Gudmundsson H., Guo J., Helm V., Hofstede C., Howat I., Humbert A., Jokat W., Karlsson N. B., Lee W. S., Matsuoka K., Millan R., Mouginot J., Paden J., Pattyn F., Roberts J., Rosier S., Ruppel A., Seroussi H., Smith E. C., Steinhage D., Sun B., Broeke M. R. V. D., Ommen T. D. V., Wessem M. V., Young D. A. 2020: *Deep glacial troughs and stabilizing ridges unveiled beneath the margins of the Antarctic ice sheet*. Nat Geosci ;13:132-7. doi.org/10.1038/s41561-019-0510-8.

Mouginot J., Rignot E., Scheuchl B., Millan R. 2017: *Comprehensive Annual Ice Sheet Velocity Mapping Using Landsat-8, Sentinel-1, and RADARSAT-2 Data*. Remote Sens (Basel) ;9:364. doi.org/10.3390/rs9040364.

Rignot E., Jacobs S., Mouginot J., Scheuchl B. 2013: *Ice-Shelf Melting Around Antarctica*. Science ;341:266-70. doi.org/10.1126/science.1235798.

Rignot E., Mouginot J., Scheuchl B. 2011a: *Antarctic grounding line mapping from differential satellite radar interferometry*. Geophys Res Lett ;38:n/a-n/a. doi.org/10.1029/2011gl047109.
Rignot E., Mouginot J., Scheuchl B. 2011b: *Ice Flow of the Antarctic Ice Sheet*. Science ;333:1427-30. doi.org/10.1126/science.1208336.

Rignot E., Mouginot J., Scheuchl B., van den Broeke M., van Wessem M. J., Morlighem M. 2019: *Four decades of Antarctic Ice Sheet mass balance from 1979–2017*. Proceedings of the National Academy of Sciences ;116:1095-103. doi.org/10.1073/pnas.1812883116.

Smith B., Dickinson S., Harbeck K., Neumann T., Hancock D., Lee J., Jelly B. 2021: *Algorithm Theoretical Basis Document (ATBD) for Land Ice Along-Track Height Products Part 2: Land-ice H(t)/ATL11*. Goddard Space Flight Center. Greenbelt, Maryland.

Smith B., Fricker H. A., Holschuh N., Gardner A. S., Adusumilli S., Brunt K. M., Csatho B., Harbeck K., Huth A., Neumann T., Nilsson J., Siegfried M. R. 2019: *Land ice height-retrieval algorithm for NASA's ICESat-2 photon-counting laser altimeter*. Remote Sens Environ ;233:111352. doi.org/10.1016/j.rse.2019.111352.